Sustainability in Civil Engineering Journal
Volume 1, Number 1, 2026
P-ISSN: xxxx-xxxx E-ISSN : xxxx-xxxx
Open Access: https://journalcendekia.com/SICEJ

Characteristics of Intraslab Earthquake Waves

Yafen Heltri Martu[1], Rusnardi Rahmat Putra[2]
[1] Faculty of Engineering, Universitas Negeri Padang
[2] Faculty of Engineering, Universitas Negeri Padang

Correspondence: yafenmartu3@gmail.com

Article Info
Article history:
Received March 06th, 2026
Revised March 09th, 2026
Accepted March 10th, 2026

Keyword:
Intraslab; Akselerograf; Response Spectrum; Arias Intensity.

ABSTRACT
Earthquakes frequently occur in Indonesia and can cause significant damage, especially in high-risk areas such as West Sumatra. One type of potentially dangerous earthquake is the intraslab earthquake, which occurs within the subducting plate at depths of 50-300km. this study aims ti identify the characteristics of infraslab earthquakes in West Sumatra and their potential impacts. The data consists of 100 earthquake events from 2008-2015, including 24 intraslab earthquakes. A quantitative analysis was conducted using MATLAB and QGIS. The results show that Peak Ground Acceleration (PGA) for the horizontal component ranges from 0.98 to 36 Gal, and from 1.07 to 10 Gal for the vertical component. The frequency content of the earthquakes ranges from 0.6 to 21 Hz (period 0.05-1.76 seconds). This indicates that intraslab earthquakes have the potential to generate significant seismic loads even though their sources are located within the tectonic plate. The highest Peak Spectral Acceleration (PSA) recorded is 0.431g, and the lowest is 0.004g. The maximum Arias Intensity is around 0.045 cm/s, which is considered moderate. This study provides insights into the seismic hazards of intraslab earthquakes as a basis for disaster mitigation in earthquake-prone areas.

INTRODUCTION

Indonesia is one of the countries with the highest levels of seismic activity in the world. In recent years, numerous earthquakes have occurred, resulting in substantial material losses and significant numbers of casualties. At present, no method is capable of accurately precting the location, timing, and magnitude of earthquakes, making seismic events a serious and persistent challenge. Therefore, scientific research is required to estimate earthquake potential by identifying high-risk areas based on historical seismic occurrences [1]. West Sumatra, which lies along the Sumatran subduction zone, has a long history of seismic activity, including earthquakes originating from intraslab sources.

Intraslab earthquakes, also known as Benioff or intraplate earthquakes, occur within the subducting slab and are generally associated with slab pull forces and normal faulting caused by tensile stress within the descending plate. This type of tectonic earthquake typically occurs at depths ranging from approximately 50 to 300 km. Intraslab seismic events are generated by subduction processes [2]. One of the primary challenges in studying intraslab earthquakes is the limited understanding of the characteristics of the seismic waves they produce. Intraslab earthquakes tend to generate high-amplitude ground motions with broader frequency spectra, which can significantly increase the potential for surface damage [3]. Moreover, intraslab earthquakes may trigger subsequent seismic events, either along the megathrust zone or within the shallow crust. This phenomenon highlights the need to better understand the dynamic interactions between intraslab earthquakes and surrounding seismic activity.

This topic is critically important because intraslab earthquakes pose considerable risks to human safety, infrastructure, and the environment. For instance, the intraslab earthquake that occurred on January 4, 2009, with a magnitude of 7.4 Mw at a depth of approximately 600 km, generated strong ground shaking that was felt in Padang, West Sumatra[4]. The intense vibrations caused widespread structural damage, including building collapses and cracked road surfaces. A deeper understanding of the characteristics of intraslab seismic waves is therefore expected to contribute to improved earthquake prediction models, enhanced earthquake-resistant structural design, and more effective disaster mitigation policies[5].

This study aims to analyze earthquake characteristics based on accelerogram data using MATLAB software. The application is employed to process and evaluate key seismic parameters, including Peak Ground Acceleration (PGA), Peak Ground Velocity (PGV), and Peak Ground Displacement (PGD), as well as to identify response spectra and seismic energy intensity. Furthermore, this research examines the impacts generated by intraslab earthquakes based on their distinctive ground motion characteristics[6].

RESEARCH METHODS

This study employes descriptive research with a quantitative approach for data analysis. The data were obtained from accelerograph sensors installed in Padang City and Bukittinggi City, distributed across five sensor locations, namely UNP, UNAND, Kuranji, the West Sumatra Governor's Office, and Bukittinggi. This research primarly utilizes secondary data. The secondary data sources include:

1. Historical earthquake recordings from accelerograph sensors covering the period 2008-2015.
2. Earthquake parameters obtained from the USGS earthquake catalog
3. Maps and parameters of the Sumatra Subduction Zone provided by the National Center for Earthquake Studies.

In this study, MATLAB is used to analyze ground acceleration data, while QGIS is employed to map the spatial distribution of intraslab earthquakes[7]. The earthquake recordings are first processed in MATLAB and correted using baseline correction and band-pass filtering to remove background noise. Subsequently, several parameters are analyzed, including amplitude, frequency content, Arias intensity, and response spectra. Spectral analysis is conducted based on the Fast Fourier Transform (FFT) concept to determine frequency-related parameters[8]. The overall research workflow is illustrated in the following research flowchart.

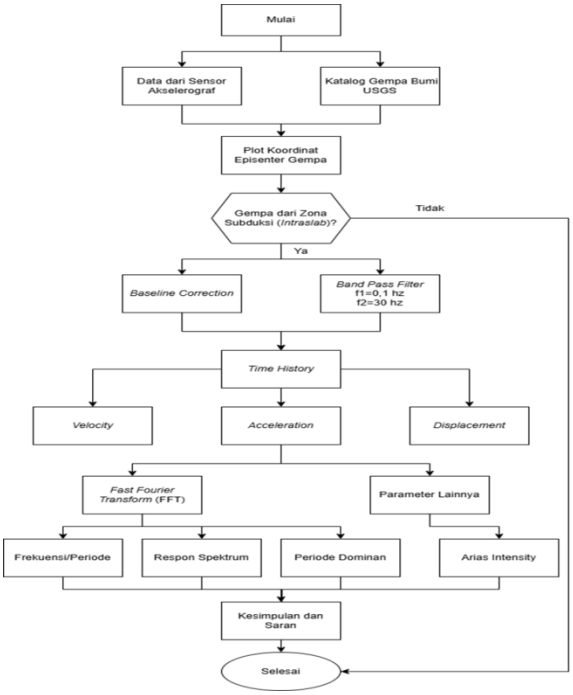

Picture 1. Research Flow Diagram

RESULTS AND DISCUSSION

This study utilizes MATLAB to analyze ground acceleration data and QGIS to map the spatial distribution of intraslab earthquakes[9]. The dataset consists of 100 earthquake events recorded between 2008 and 2015, of which 24 events are classified as intraslab earthquake. The spatial distribution map of the 24 intraslab earthquakes, based on accelerograph sensor records, is presented in the following figure.

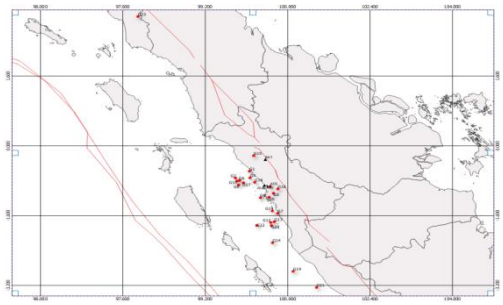

Picture 2. Intraslab Earthquake Distribution Map

1. Earthquake data analysis using MATLAB

The earthquake data obtained from accelerograph sensors were analyzed using MATLAB by implementing mathematical formulations within the program to compute the required earthquake parameters.

```
clear all
clc

% Mengidentifikasi data rekaman gempa
data=load('UNP_10-09-11_16.33.15 arah x1000.txt');
t=data(:,1);    % data kolom waktu
a_t=data(:,2);  % data kolom acceleration

% Koreksi baseline menggunakan metode polinomial
order = 1;                  % bisa disesuaikan
p = polyfit(t, a_t, order);       % fitting baseline
baseline = polyval(p, t);         % evaluasi baseline di titik x
a_t_corrected = a_t - baseline;   % kurangi sinyal dengan baseline

% 2. Parameter dasar
Order=4;
Dt = mean(diff(t)); % Menghitung selisih waktu rata-rata (interval sampling)
Fs = 1/Dt;                  % Menentukan frekuensi sampling
f_low = 0.1;                % Frekuensi cut-off bawah (Hz)
f_high = 30;                % Frekuensi cut-off atas (Hz)

% Normalisasi frekuensi cut-off terhadap Nyquist Frequency
Wn = [f_low f_high] / (Fs/2);  % Normalisasi terhadap Nyquist

% Desain filter Butterworth band-pass
[b, a] = butter(Order, Wn, 'bandpass');

% Terapkan filter (menggunakan filtfilt untuk menghindari phase shift)
acc_filtered = filtfilt(b, a, a_t_corrected);
```

Picture 3. Matlab Code

2. Grouping the analysis results based on parameters

The MATLAB program produces several earthquake parameters, including Peak Ground Acceleration (PGA), Peak Ground Velocity (PGV), Peak Ground Displacement (PGD), Fourier amplitude, Arias intensity, and response spectra. These results are then grouped according to each parameter, and the maximum values are determined for each category. The outcomes are subsequently presented in the form of tables and graphs.

Earthquake Amplitude:

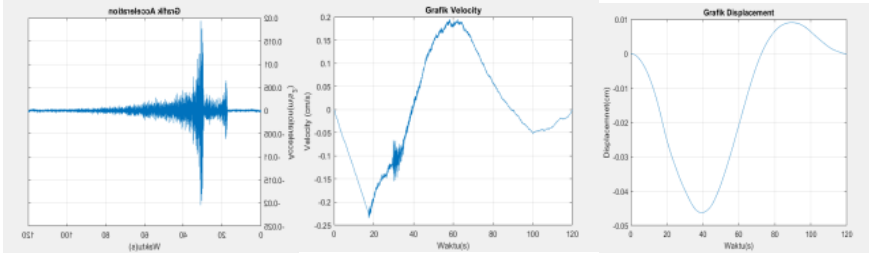

Picture 4. Graphs PGA, PGV, and PGD X-direction

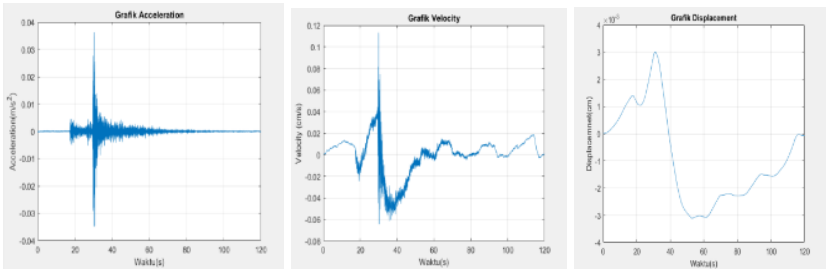

Picture 5. Graphs PGA, PGV, and PGD Y-direction

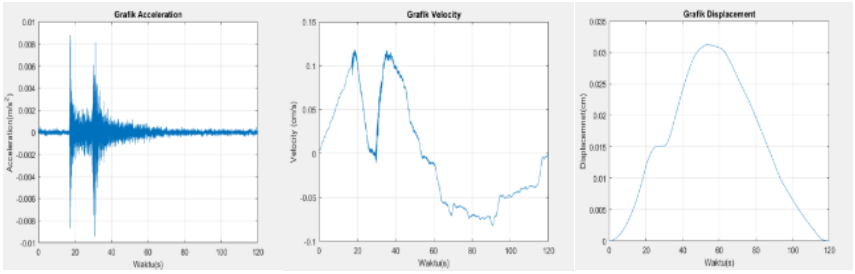

Picture 6. Graphs PGA, PGV, and PGD Z-direction

The PGA values range from 0.98 to 36 Gal for the horizontal components and from 1.07 to 10 Gal for the vertical component. The highest PGA was recorded at G1 on the Y component, reaching 36.00 Gal. the maximum PGV values was observed at G14 (ADS, Mw 5.3; R = 94 km), with a value of 0.983 cm/s on the Y component. Meanwhile, the highest PGD value was identified at G15 (ADS, Mw 5.1; R = 150 km) on the X component, with a magnitude of 0.211 cm.

These values indicate the possible presence of local anomalies, such as site effects or local amplification associated with soft soil conditions. The influence of source-to-site distance on ground motion intensity is also highly significant. As seismic energy attenuates with increasing distance from the source, PGA, PGV, and PGD values decrease accordingly.

Furthermore, the type and sensitivity of sensors contribute to data variability. For example, the ADS sensor in events G5 and G7 (Mw 5.3-5.5) recorded relatively higher PGA and PGV values compared to the KRJ sensor in events G3 and G6, despite having similar magnitudes and source distances.

Frequency:

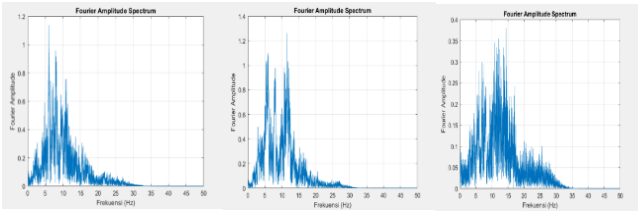

Picture 7. Graphs Fourier Amplitude Components X,Y, Z

the recorded frequency (F) values range from a minimum of 0.64 Hz (G23, X component) to a maximum 0f 21.44 Hz (G21, Z component).

Findings:

Most earthquakes exhibit dominant frequencies between 3 and 12 Hz, indicating rapid oscillations that still fall within the resonance range of low- to mid – rise buildings. Event G21 shows an exceptionally high dominant frequency on the Z component (21.44 Hz), suggesting the presence of sharp local vibrations.

The dominant period (T) is defined as the time required for a frequency wave to complete one full oscillation cycle (in seconds, s). the dominant period values range from a shortest period of 0.046 s (G21, X component) to a longest period of 1.76 s (G23, X component).

Findings:

Most dominant periods are relatively short (< 0.3s), indicating the predominance of short-period waves. However, event G23 exhibits an extremely long dominant period (up to 1.76 s), which may pose a significant hazard to high-rise buildings due to potential resonance effects.

Spectrum Response

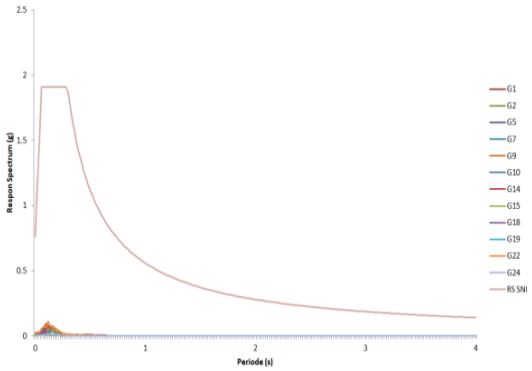

Picture 8. Eartquake Spectrum Response with RS SNI 1726 2019 Component X

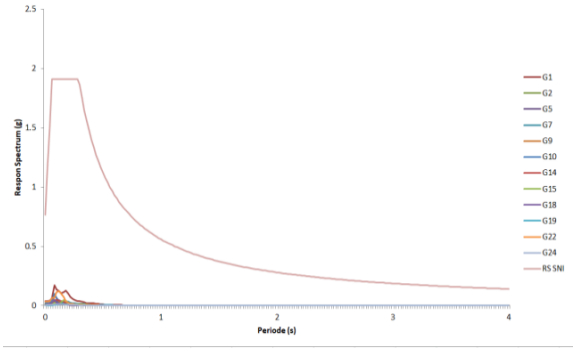

Picture 9. Eartquake Spectrum Response with RS SNI 1726 2019 Component Y

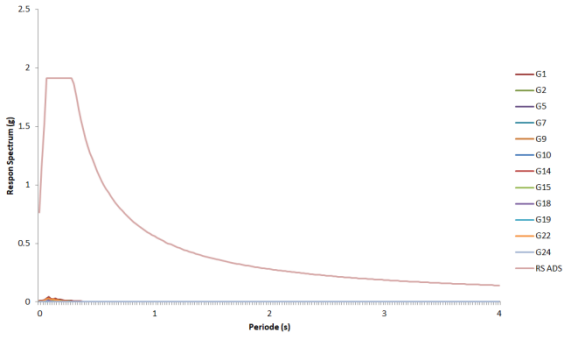

Picture 10. Eartquake Spectrum Response with RS SNI 1726 2019 Component Z

The recorded Peak Spectral Acceleration (PSA) values range from a minimum of 0.004 g (G21, Z component) to a maximum of 0.431 g (G19, Z component). These values fall within the light to moderate seismic intensity category, which is generally considered safe for structures that are properly designed to be earthquake-resistant. However, in regions such as Padang, which are characterized by soft coil conditions and a wide variety of building types, PSA values exceeding 0.1 g require special attention, as they may lead to soil amplification effects and cause light to moderate damage to simple structures.

Based on the response spectra, several events-namely G1, G2, G3, and G4- exhibit PSA values exceeding 0.1 g within the frequency range of 1-3 Hz, which may include light to moderate damage to conventional building structures lacking seismic damping systems. This finding indicates that intraslab earthquakes have the potential to generate significant seismic loads, even though their sources are located within the subducting slab [10]

Arias Intensity :

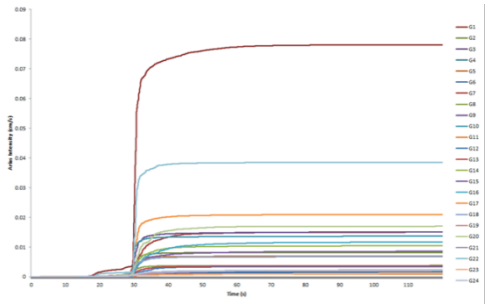

Picture 11. Arias Intensity Graph of Component X

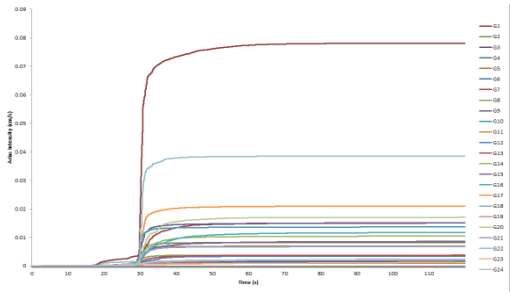

Picture 12. Arias Intensity Graph of Component Y

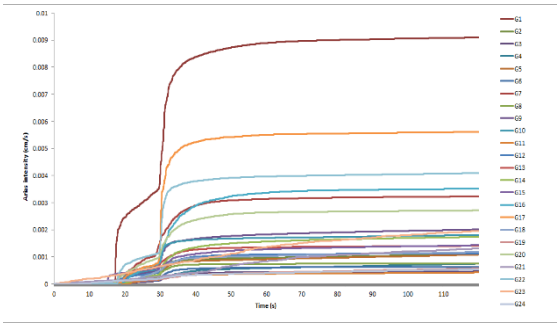

Picture 13. Arias Intensity Graph of Component Z

Most of the curves begin to rise sharply between 25 and 35 seconds, indicating the occurrence of the main shock, during which seismic energy is released significantly. After this phase, the curves tend to level off, signifying that the earthquake has subsided and no substantial additional energy is being released. Differences in curve heights reflect variations in earthquake strength; for example, the G1 curve (red) reaches the highest value, indicating that it represents the event with the largest energy release. In contrast, curves with lower amplitudes correspond to weaker or shorter-duration earthquakes. Steep curve shapes indicate rapid and abrupt energy release, whereas gentler slopes suggest a slower and more gradual release of seismic energy.

This graph is highly useful in earthquake engineering studies as it provides a clear depiction of the intensity and duration of seismic energy experienced by a region or structure. The maximum Arias Intensity value observed in the graph (≈ 0.780 cm/s) is generally classified as moderate and not extreme. However, for areas such as Padang City, which are characterized by soft soil conditions and a high proportion of non-engineered buildings, this value may still pose a significant risk, particularly for structures that are not designed to be earthquake-resistant.

Table 1. Earthquake Characteristics of The Sumatra Subduction Zone (Intraslab)

No	Sensor	Mw	R (km)	Komponen	PGA (Gal)	PGV (cm/s)	PGD (cm)	F (Hz)	T (s)	PSA (g)	Tp (s)	AI (cm/s)
G1	ADS	5,4	124	X	20,11	0,23	0,046	6,00	0,166	0,096	0,100	0,43
				Y	36,00	0,11	0,031	11,51	0,086	0,170	0,080	0,78
				Z	9,12	0,11	0,031	14,39	0,069	0,045	0,080	0,09
G2	ADS	5	118	X	15,99	0,93	0,086	7,76	0,128	0,067	0,120	0,12
				Y	14,51	0,75	0,160	5,77	0,173	0,050	0,100	0,08
				Z	3,13	0,16	0,042	7,40	0,135	0,128	0,100	0,01
G3	KRJ	5,5	104	X	3,33	0,55	0,087	3,04	0,328	0,011	0,200	0,01
				Y	6,37	0,27	0,043	3,36	0,297	0,191	0,120	0,01
				Z	1,37	0,38	0,047	3,01	0,331	0,005	0,240	0,00
G4	UNP	5,4	106	X	5,59	0,51	0,062	6,24	0,160	0,189	0,140	0,01
				Y	3,92	0,35	0,082	6,12	0,163	0,025	0,160	0,017
				Z	1,56	0,11	0,023	4,13	0,242	0,005	0,140	0,00
G5	ADS	5,3	102	X	28,44	0,47	0,073	8,14	0,122	0,037	0,100	0,06
				Y	10,88	0,69	0,135	8,33	0,119	0,046	0,120	0,06
				Z	9,90	0,41	0,080	10,98	0,091	0,011	0,100	0,01
G6	KRJ	5,5	112	X	4,90	0,31	0,060	2,41	0,414	0,012	0,080	0,01
				Y	4,31	0,61	0,073	6,22	0,160	0,014	0,160	0,01
				Z	2,35	0,30	0,053	2,86	0,348	0,009	0,080	0,00
G7	ADS	5,5	112	X	14,22	0,20	0,045	8,61	0,116	0,061	0,100	0,22
				Y	11,47	0,17	0,023	11,23	0,089	0,032	0,080	0,150
				Z	36,29	0,25	0,037	14,29	0,069	0,014	0,060	0,03
G8	KRJ	5,4	89	X	6,18	0,57	0,105	3,47	0,287	0,023	0,140	0,02
				Y	9,51	0,36	0,052	3,35	0,298	0,028	0,180	0,03
				Z	2,55	0,93	0,162	4,72	0,211	0,007	0,080	0,00
G9	ADS	5,5	105	X	15,79	0,15	0,032	7,55	0,132	0,058	0,120	0,12
				Y	16,87	0,72	0,123	10,36	0,096	0,076	0,080	0,15
				Z	4,12	0,13	0,032	10,21	0,097	0,017	0,100	0,02
G10	ADS	5,4	107	X	18,05	0,10	0,019	7,76	0,128	0,077	0,140	0,13
				Y	19,22	0,14	0,019	11,62	0,086	0,099	0,080	0,13
				Z	4,31	0,18	0,021	16,47	0,060	0,023	0,080	0,01
G11	KRJ	5,3	75	X	2,06	0,25	0,051	3,97	0,251	0,007	0,140	0,00
				Y	3,92	0,96	0,176	6,37	0,156	0,010	0,120	0,00
				Z	1,47	0,18	0,035	1,21	0,823	0,006	0,060	0,00
G12	KRJ	5,6	119	X	4,61	0,38	0,042	3,93	0,254	0,020	0,120	0,02
				Y	5,19	0,44	0,071	3,55	0,281	0,018	0,140	0,03
				Z	2,45	0,18	0,028	3,30	0,302	0,009	0,080	0,01
G13	KRJ	5,6	118	X	4,61	0,23	0,041	5,99	0,166	0,016	0,180	0,02
				Y	5,78	0,69	0,069	3,54	0,282	0,021	0,280	0,03
				Z	2,84	0,34	0,074	4,74	0,210	0,009	0,200	0,01
G14	ADS	5,3	94	X	17,95	0,16	0,034	7,75	0,129	0,078	0,120	0,14
				Y	11,08	0,98	0,209	10,76	0,092	0,050	0,100	0,103
				Z	3,33	0,15	0,039	16,72	0,059	0,013	0,120	0,01
G15	ADS	5,1	150	X	3,23	0,57	0,106	8,02	0,124	0,012	0,120	0,10
				Y	3,92	0,28	0,037	8,28	0,120	0,012	0,120	0,08
				Z	0,98	0,99	0,211	14,65	0,068	0,004	0,060	0,01
G16	GBR	5,7	104	X	12,65	0,23	0,061	8,66	0,115	0,055	0,120	0,12
				Y	10,39	0,10	0,022	11,30	0,088	0,034	0,120	0,11
				Z	4,51	0,42	0,099	3,75	0,266	0,014	0,140	0,03
G17	GBR	5,5	90	X	18,73	0,76	0,131	7,62	0,131	0,074	0,100	0,16
				Y	28,74	0,80	0,095	3,26	0,306	0,063	0,120	0,20
				Z	9,90	0,65	0,145	3,25	0,307	0,030	0,240	0,056
G18	ADS	5,3	67	X	5,19	0,20	0,042	10,57	0,094	0,024	0,080	0,03
				Y	8,04	0,10	0,021	12,84	0,077	0,049	0,080	0,06
				Z	2,35	0,14	0,026	17,24	0,058	0,097	0,080	0,01
G19	ADS	5	234	X	4,21	0,11	0,018	5,92	0,168	0,013	0,240	0,02
				Y	2,64	0,04	0,005	5,02	0,199	0,011	0,260	0,02
				Z	1,17	0,04	0,005	3,78	0,264	0,064	0,360	0,05
G20	GBR	5,5	120	X	10,30	0,21	0,049	10,31	0,111	0,042	0,120	0,11
				Y	12,94	0,05	0,011	11,59	0,086	0,055	0,080	0,16
				Z	3,53	0,38	0,082	21,44	0,046	0,012	0,060	0,027

G21	UNP	5,4	290	X	1,86	0,14	0,029	1,03	0,967	0,006	0,180	0,02
				Y	2,15	0,06	0,010	1,04	0,960	0,008	0,960	0,02
				Z	1,07	0,16	0,023	1,05	0,944	0,004	0,920	0,01
G22	ADS	5,5	119	X	24,72	0,10	0,018	8,16	0,122	0,113	0,120	0,31
				Y	30,70	0,10	0,017	8,56	0,116	0,123	0,120	0,03
				Z	8,43	0,09	0,160	8,63	0,115	0,031	0,080	0,04
G23	BKT	6,7	517	X	1,17	0,02	0,002	0,79	1,76	0,005	1,200	0,01
				Y	0,98	0,03	0,006	0,80	1,23	0,003	0,740	0,01
				Z	1,17	0,08	0,015	0,64	1,55	0,003	1,220	0,01
G24	ADS	5,1	163	X	3,23	0,05	0,010	8,01	0,124	0,012	0,120	0,02
				Y	3,72	0,02	0,003	8,29	0,120	0,012	0,120	0,02
				Z	1,07	0,099	0,021	14,65	0,058	0,004	0,060	0,00

CONCLUSION

The following conclusions can be drawn from the time-history analysis of strong ground motion in both the time domain and the frequency domain:

1. The Peak Ground Acceleration (PGA) values range from 0.98 to 36 Gal for the horizontal components and 1.07 to 10 Gal for the vertical component. These PGA values are influenced by the hypocentral distance between the earthquake source and the sensor, local soil conditions, and the relatively small earthquake magnitudes.
2. The average frequency content of the analyzed intraslab earthquakes ranges from 0.6 to 21 Hz, corresponding to dominant periods of 0.05 to 1.75 seconds.
3. The Peak Spectral Acceleration (PSA) values range from a minimum of 0.004 g (G21, Z component) to a maximum of 0.431 g (G19, Z component). These values fall within the light to moderate seismic intensity category, which is generally considered safe for structure designed to be earthquake-resistant.
4. The response spectra recorded at each sensor location, when compared with the Indonesian Earthquake Design Response Spectrum (EDRS) specified in SNI 1726:2019, remain well below the design spectrum, indicating a safe condition.
5. The maximum Arias Intensity observed in the graph (≈ 0.045 cm/s) is classified as moderate and not extreme. However, in areas such as Padang City, which are characterized by soft soil conditions and a high proportion of non-engineered buildings, this value may still pose a potential risk, particularly for structures that are not designed to be earthquake-resistant.

REFERENCES

[1] W. Erlangga, “KARAKTERISTIK DAN PARAMETER SUBDUKSI SUMBER GEMPA PULAU JAWA,” vol. XXV, no. 2, 2020.

[2] Santoso and A.Soehaimi, “Geo-Hazards,” 2010.

[3] S. Koesuma, V. Fajrin, and B. Sunardi, “IDENTIFIKASI ZONA BAHAYA GEMPA BUMI BERDASARKAN PERCEPATAN TANAH MAKSIMUM DI KOTA SEMARANG,” *Indonesian Journal of Environment and Disaster (IJED)*, vol. 1, no. 2, pp. 65–72, 2022, [Online]. Available: https://earthquake.usgs.gov/data/VS30/

[4] F. Raharjo, “ESTIMASI MODEL PERCEPATAN TANAH MAKSIMUM UNTUK SUMBER GEMPABUMI DI INTERFACE DAN INTRA-SLAB SUBDUKSI UNTUK JENIS TANAH LUNAK DI KOTA PADANG MENGGUNAKAN MODEL ATTENUASI LIN DAN LEE,” *Megasains*, vol. 13, no. 01, pp. 19–23, Aug. 2022, doi: 10.46824/megasains.v13i01.80.

[5] D. H. Natawidjaja, “The Sumatran Fault Zone-from Source to Hazard,” 2007.

[6] C. Rajaram and R. Pradeep Kumar, “Correlation between building damage, ground motion parameters and input energy: a novel ranking scheme using multivariate analysis,” 2023.

[7] T. A. Aquib, J. Sivasubramonian, and P. M. Mai, “Analysis of Ground Motion Intensity Measures and Selection Techniques for Estimating Building Response,” *Applied Sciences (Switzerland)*, vol. 12, no. 23, Dec. 2022, doi: 10.3390/app122312089.

[8] A. Riyani, A. Nurrochman, E. Sanjaya, P. Rizqiyah, and A. Junaidi, "Journal of Informatics, Information System, Software Engineering and Applications Mengidentifikasi Sinyal Suara Manusia Menggunakan Metode Fast Fourier Transform (Fft) Berbasis Matlab," vol. 1, no. 2, pp. 42–050, 2019, doi: 10.20895/INISTA.V1I2.

[9] P. Ezrahayu, "Penggunaan Aplikasi QGIS Processing Modeler dalam Menentukan Potensi Bencana Tanah Longsor di Kabupaten Bogor," *Geodika: Jurnal Kajian Ilmu dan Pendidikan Geografi*, vol. 8, no. 1, pp. 41–52, May 2024, doi: 10.29408/geodika.v8i1.25729.

[10] Kadnan, "HUBUNGAN EMPIRIS INTENSITAS SEISMIK DENGAN PARAMETER GETARAN TANAH DI WILAYAH JAWA BARAT."